EEET ECOLOGICAL ENGINEERING & ENVIRONMENTAL TECHNOLOGY

Ecological Engineering & Environmental Technology 2023, 24(8), 272–292
https://doi.org/10.12912/27197050/172569
ISSN 2719-7050, License CC-BY 4.0

Received: 2023.09.01
Accepted: 2023.09.19
Published: 2023.10.15

Landslide Hazard Assessment in the Heterogeneous Geomorphological and Environmental Context of the Rif Region, Morocco – A Machine Learning Approach

Maryem Hamidi[1*], Tarik Bouramtane[1], Shiny Abraham[2], Ilias Kacimi[1], Laurent Barbiero[3], Nadia Kassou[1], Vincent Valles[4], Gad Levy[5]

[1] Geosciences, Water and Environment Laboratory, Faculty of Sciences, Mohammed V University, Avenue Ibn Batouta, Rabat 10100, Morocco

[2] Electrical and Computer Engineering Department, Seattle University, Seattle, WA 98122, USA

[3] Géoscience Environnement Toulouse, IRD, CNRS, UPS, OMP, Mixed Research Unit 5563, 14 Av. E. Belin, 31400 Toulouse, France

[4] Mixed Research Unit EMMAH (Environnement Méditerranéen et Modélisation des Agro-Hydrosystèmes), Hydrogeology Laboratory, Avignon University, 84916 Avignon, France

[5] NorthWest Research Associates & Pan Ocean Remote Sensing Association, Seattle, WA 98105, USA

* Corresponding author's e-mail: maryem_hamidi@um5.ac.ma

ABSTRACT

Landslides are considered to be one of the most significant and critical natural hazards in the heterogeneous geomorphological setting of the Rif region of Morocco. Despite the high susceptibility to landslides, the region lacks detailed studies. Therefore, this research introduces four advanced machine learning methods, namely Support Vector Machine (SVM), Classification and Regression Trees (CART), Multivariate Discriminant Analysis (MDA), and Logistic Regression (LR), to perform landslide susceptibility mapping, as well as study of the connection between landslide occurrence and the complex regional geo-environmental context of Taounate province. Fifteen causative factors were extracted, and 255 landslide events were identified through fieldwork and satellite imagery analysis. All models performed very well (AUC > 0.954), while the CART model performed the best (AUC= 0.971). However, SVM demonstrated superior performance compared to other methods, achieving the highest accuracy (89.92%) and F1-measure (81.66%) scores on the training data, and the highest accuracy (83.01%), precision (81.74%), and specificity (79.46%) scores on the test data. The results do not necessarily indicate that LR and MDA have the lowest predictive ability, as they demonstrated high accuracy in terms of AUC and in some classification tasks. Moreover, they provide the significant advantage of easy interpretation of the geo-environmental processes that control landslides. Rainfall is the primary triggering factor of landslides in the study area. The majority of landslides occurred on slopes, particularly those located along rivers and faults, suggesting that landslides in the region are closely associated with active tectonics and precipitation. All four models predicted similar spatial distribution patterns in landslide susceptibility. The results showed that almost half of the area mainly in the north and northwest, has a very high susceptibility to landslides. The findings provide valuable references for land use management and the implementation of effective measures for landslide prevention.

Keywords: landslide, machine learning, Morocco, susceptibility mapping, remote sensing, Rif.

INTRODUCTION

Landslides pose a significant danger in various mountainous regions around the globe and can result in devastating consequences such as loss of property, economic instability, and loss of life (Prasad & Francescutti, 2017). The destructive impact of landslides is increasing globally due to deforestation, global population growth, and climate change, whereby the latter alters the stability of slopes and bedrock through changes in precipitation and/or temperature (Saha et al., 2021). Landslides can be local and superficial but could also occur on a large scale and suddenly, affecting the slopes of entire catchments and leading to severe landscape damage. Therefore, understanding the dynamics of landslides and developing effective mitigation measures are essential for minimizing the impact of these hazard events and ensuring the safety of vulnerable populations and infrastructure.

Africa, notably, stands out as a significant landslide-prone area due to high population growth and the influence of climate change, resulting in increased precipitation and more frequent and violent rainstorms (Broeckx et al., 2018; Gariano & Guzzetti, 2016). The tectonically active region extending from Morocco to Egypt contributes to the heightened susceptibility of the northern margin of Africa to landslides (Poggi et al., 2020). Despite the critical necessity for landslide susceptibility mapping in North Africa, only a few studies have been conducted, and the majority of them have focused on Morocco (Abdı et al., 2021; Anis et al., 2019). Integrating landslide susceptibility mapping into the disaster management plans of each exposed country is crucial for improving disaster management and mitigation strategies (P. Zhao et al., 2022).

The Taounate province in Northern Morocco is prone to numerous landslides and is located within the geologically diverse Intra and Mesorif domains, as well as the geologically consistent Prerif region. A recent study has identified over 1,000 landslide cases in Taounate alone, equivalent to 25 movements/km2 (Abidi et al., 2019). The geology of this area, characterized by active tectonics and rugged terrain, and its climate, characterized by long periods of drought followed by periods of heavy precipitation in the form of extreme events, are considered the leading causes of this natural hazard (Benabdelouahab et al., 2020). Moreover, all the studies conducted to generate landslide susceptibility maps are case-by-case studies and do not cover the entire province. For instance, investigations by Jemmah & Brahim, 2018, and the research conducted by Benchelha et al., 2020, focused on the province's northern regions, where they performed a comparative assessment of various techniques for mapping landslide susceptibility. Nevertheless, previous research efforts have not adequately addressed the overall complexities of the entire region under study. Producing clear maps is essential in mapping landslide susceptibility, and various techniques have been suggested and utilized for this aim, including qualitative and quantitative approaches. Qualitative methods require an expert to estimate landslide potential and slope movement. On the other hand, quantitative methods, such as statistical or probabilistic techniques, have proven effective in identifying areas that require intervention or development and are used by policymakers with input from scientists, engineers, and the general population (Bravo-López et al., 2022; Reichenbach et al., 2018).

Numerous statistical techniques have been used in order to generate landslide susceptibility maps in the Moroccan Rif region. For example, Hierarchical Fuzzy Inference Systems (HFIS) that were applied in the Rif Mountains' center region (Ozer et al., 2020) and fuzzy Analytical Hierarchy Process (FAHP) were combined for landslide susceptibility modeling in southeast Morocco (Sadiki et al., 2023); Weight Of Evidence (WOE) was applied in Tetouan-Ras Mazar (Elmoulat & Ait Brahim, 2018), an area of the Rif chain (Es-smairi et al., 2021) and Taounate-Ain Aicha (Jemmah & Brahim, 2018). Logistic regression (LR) was used in Taounate-Oudka and the Sahla catchment area (El-Fengour et al., 2021), while the Analytical Hierarchical Processes (AHP) method was applied in Tangiers (Brahim et al., 2018), the Larache Province (Hamdouni et al., 2022) and parts of the Rif mountains (Es-smairi et al., 2021). However, these methods rely on assumptions about the data, such as normality and linearity, which can limit their accuracy in analyzing complex interrelationships between different causative factors. Furthermore, reclassifying continuous causative factors to prepare the dataset can be challenging and affect the nature of the data (Chen et al., 2018), resulting in decreased model accuracy. Additionally, classical statistical methods, which require large sample sizes and are less able to process high-dimensional and complex data (He et al., 2012), The geo-environmental processes controlling landslides in the Taounate province are complicated and remain unknown, highlighting the need for further research and effort in landslide susceptibility modeling and mapping. However, there are opportunities for improvement by leveraging the strengths of high-resolution, freely available remote sensing data and the efficiency of advanced machine learning methods. Machine learning techniques have lately gained significant popularity in assessing landslide susceptibility (Rahmati et al., 2019). The accessibility of satellite imagery has enhanced machine learning's success, geographic information systems (GIS), and the scarcity of historical landslide records (Ado et al., 2022). Despite the numerous advantages offered by machine learning, including its ability to handle high-dimensional data efficiently, fit nonlinear relationships between targets and factors (X. Zhou et al., 2021), as well as its adaptability, reproducibility, and ability to quantitative analysis of factors contributing to landslide development. The use of machine learning methods for landslide susceptibility mapping has been limited in North Africa, particularly in Morocco.

Few research studies have evaluated the efficiency of Artificial Neural Networks (ANN) and LR in identifying suitable methods for limited regions within the Taounate province. In a study by Benchelha et al., 2020, the Multivariate Adaptive Regression Spline (MARSpline) model demonstrated a higher success rate compared to LR and ANN models. However, it should be mentioned that this study was verified using a single assessment measure (Area Under Curve (AUC)) and was based on eight conditioning factors. In other research, Sahrane et al., 2023 used LR and ANN models to examine the effect of landslide inventory maps on landslide susceptibility in two distinct geomorphologically different regions in Taounat province. In the Atlas Mountains, the Support Vector Machine (SVM) model outperformed the Weight of Evidence (WoE) and Radial Basis Function Network (RBFN) models despite being utilized only once in Morocco (Naceur et al., 2022). The case studies mentioned have their limitations, as the effectiveness of machine learning techniques can be influenced by the unique geo-environmental characteristics of each region, various contributing factors, and the accuracy of input data (P. Zhao et al., 2022). Hence, to ensure the generation of precise landslide susceptibility maps, it is essential to assess and contrast alternative advanced machine learning approaches capable of adequately addressing the overall study area complexities when performing landslide susceptibility mapping.

Addressing the current limitations of models used and the data gaps in Morocco's Rif mountains, we concentrated on analyzing the performance of four machine learning methods: SVM, LR, Multivariate Discriminant Analysis (MDA), and Classification and Regression Trees (CART) for landslide susceptibility mapping. These models were chosen based on a literature review and the recognition that different linear and nonlinear factors influence landslide occurrence. The aim of this research study is not limited to the assessment of machine learning models but also to develop an extensive understanding of the geo-environmental factors controlling landslides in one of the most affected and complex regions of North Africa. Moreover, the strength of this study lies in its extensive and significant database, comprising 255 landslides and 15 geo-environmental factors using remote sensing and fieldwork data. These contributions represent a substantial addition to the scientific community.

STUDY AREA

The geographical area studied covers a mountainous province of around 5616 km² in the Fez-Meknes region of North Morocco (Figure 1). In 2009, the province's population was approximately 678,000, giving it an average density of 121 inhabitants per km², relatively high for a mountainous area. The province straddles three structural subdomains of the Rif belt: Intra-Rif, Meso-Rif, and Pre-Rif, and therefore is characterized by different tectonic units and a high diversity of lithological units (limestone, marl, flysch, etc.) (Michard et al., 2014; Poujol et al., 2014). The topography is contrasted with a varied landscape due to the tectonic deformations of the region, which can be divided into two main sub-regions:

- The northern part, linked to the Rifian domain, is a mountainous relief that covers about 40% of the province's total area, with altitudes up to 1800 m. The province is crossed by several vital rivers constituting the main tributaries of the Oued Ouergha
- The southern part, linked to the pre-Rifian zone, has a hilly relief with an altitude ranging from 150 m along Oued Inaouen and 1000 m at Jbel Zeddour.

The province's climate is Mediterranean, with dry, hot summers and cold, wet winters, and annual rainfall averages around 790 mm, which can exceed 1800 mm in the Jebel Outka area. The average temperature is around 16.9 °C, which can exceed 45 °C in summer (El-Assri et al., 2021). This situation is compounded by a rising occurrence of heavy rainfall, earthquakes, and urban development, making it one of Morocco's regions most susceptible to high-impact landslides.

DATA AND METHODS

A schematic representation of the application procedure is shown in Figure 2. The main steps in the methodological approach comprise data collection and organization, the model's development and validation, and the contribution of conditioning factors.

Data collection

Generating landslide inventory map

Past and present landslides are critical indicators of future landslides (Guzzetti et al., 1999). Therefore, an inventory of landslides, based on historical data collected through exhaustive investigations by Maurer, 1968 and high-resolution Google Earth images, was utilized to create a map of landslides in the study region. Google Earth Pro software was employed to validate the existence of historical data and collect new landslide and non-landslide points. Non-landslide locations were randomly selected from areas without landslide, ensuring a minimum distance of 2000 meters from landslide sites. In order to produce a single landslide inventory map, six different types of landslides, including rockfalls, debris flows, and complicated landslides, were identified. The inventory map contained 255 landslides and 255 non-landslide points in Taounate province (Figure 1). Figure 2 illustrates the methodological process used in this study.

Generating landslide conditioning factors

The interaction of different factors causes the occurrence of a landslide. There are no specific guidelines for selecting these factors, each of which may contribute to a greater or lesser extent in different regions. However, it is commonly assumed that landslides will happen under similar conditions as in the past. (Youssef & Pourghasemi, 2021). Based on the literature assessment and the study area's environmental and geographical characteristics, fifteen landslide conditioning factors were chosen. They can be divided into four categories (Table 1, Figure 3), namely topographic (altitude, Topographic

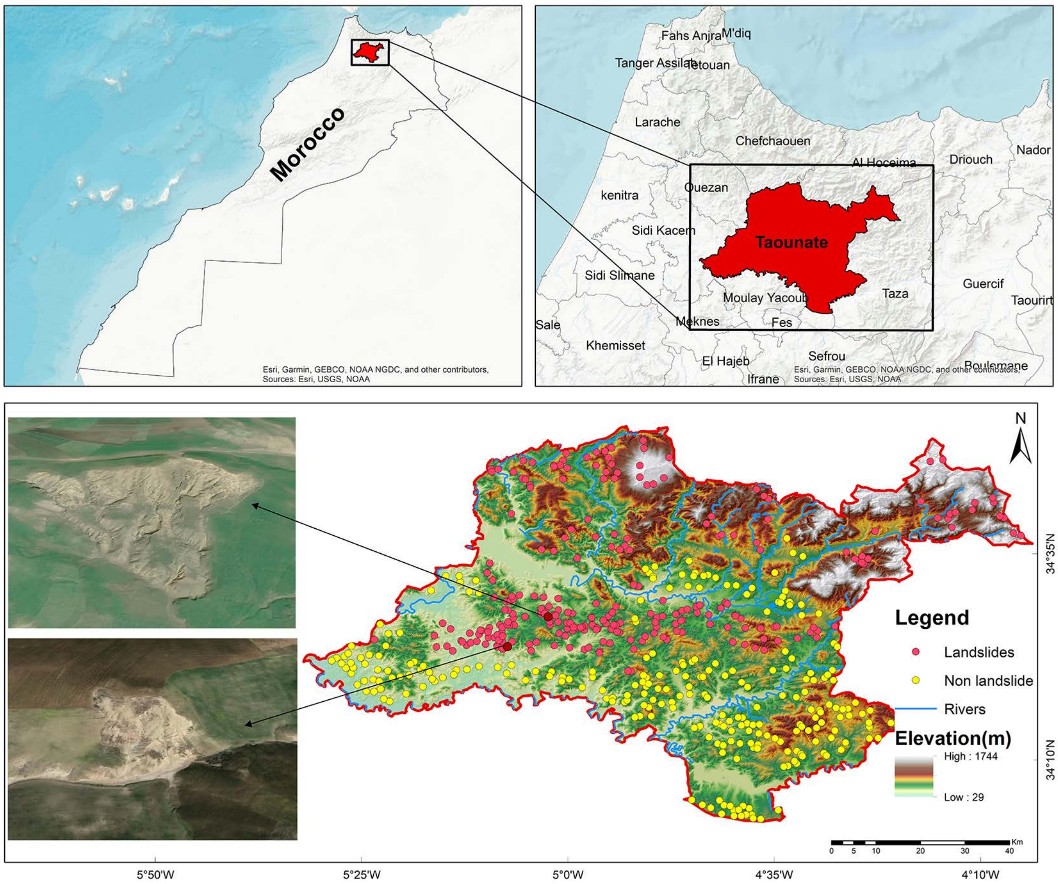

Figure 1. Location maps of the study area showing the location of landslides and non-landslide areas

Position Index (TPI), Topographic Wetness Index (TWI), slope, aspect, curvature, profile curvature, plan curvature), hydrological (precipitation, distance to river), geological (lithology, distance to faults), and land cover related (distance to roads, Land Cover and land Use (LCLU) and Normalized Difference Vegetation Index (NDVI)). The discrete variables were distributed following the properties of the data, while the topographic factors were derived using a 30 m resolution Digital Elevation Model (DEM). Using the GIS tool, all conditioning factors were converted into a raster format and synchronized at a spatial resolution of 10×10 m cell size.

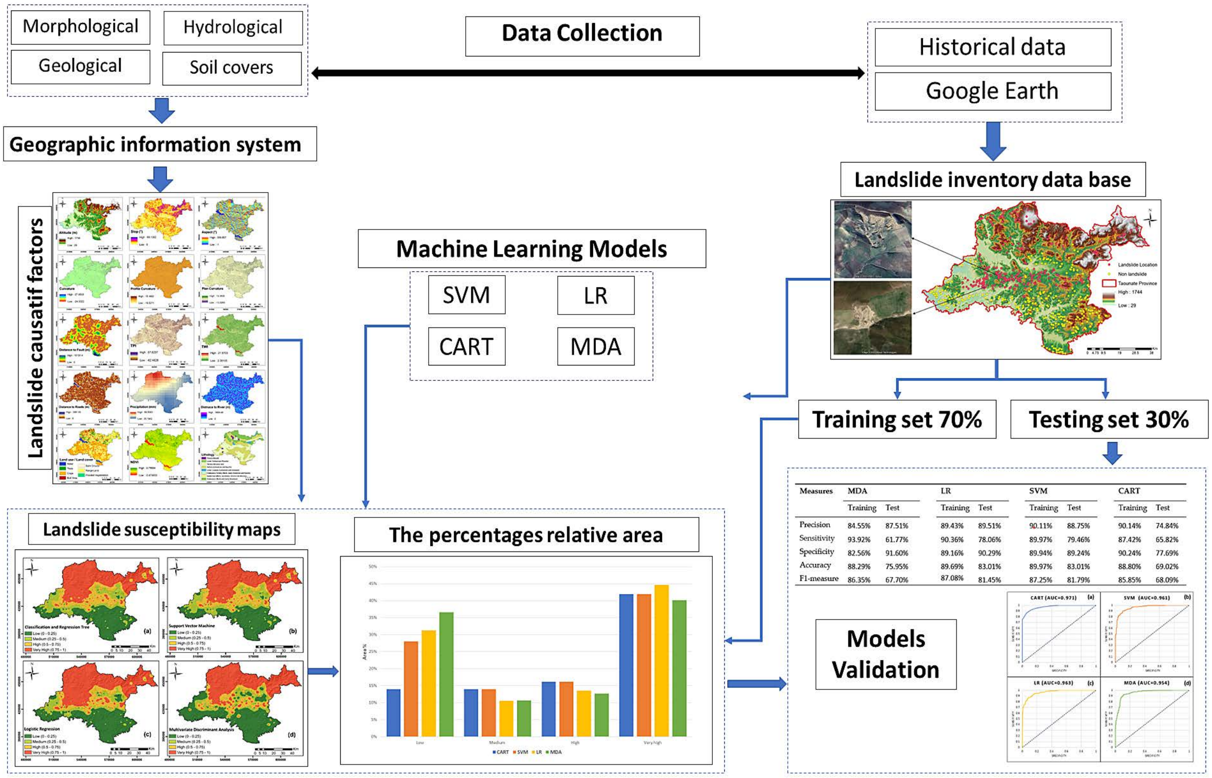

Figure 2. Methodological flowchart

Table 1. Details of landslide conditioning factor data

Cluster	Conditioning factors	Type	Data source
Topographical	Altitude	Continuous	Digital Elevation SRTM – 30 m
	Slope	Continuous	
	Aspect	Continuous	
	Curvature	Continuous	
	Profile curvature	Continuous	
	Plan curvature	Continuous	
	TPI	Continuous	
	TWI	Continuous	
Geological	Lithology	Categorical	Geological data of Africa USGS + Geological map of Morocco 1/200,000
	Distance to faults	Continuous	Geological map of Morocco 1/200,000 + satellite imagery
Hydrological	Precipitation	Continuous	CHIRPS - Satellite precipitation product (~ 5 km)
	Distance to Rivers	Continuous	Digital Elevation SRTM – 30 m
Land covers	NDVI	Continuous	Sentinel-2 time series of 2021 – 10 m
	Land cover/Land use	Categorical	Esri Land cover/land use of 2021 – 10 m
	Distance to roads	Continuous	Google Earth

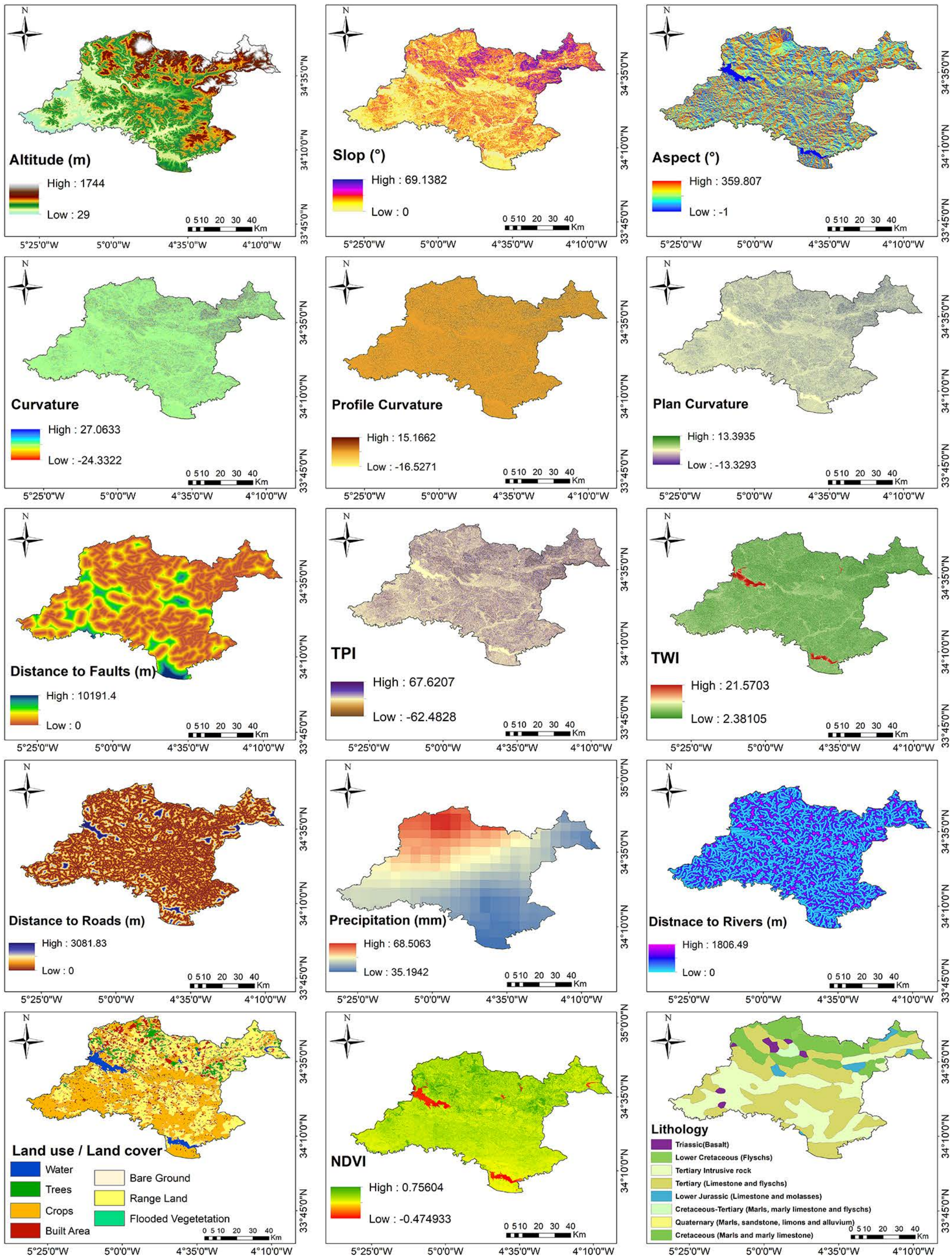

Figure 3. Landslide conditioning factors maps

Altitude

The research area's elevation ranges from 29 to 1744 meters above sea level. The altitude conditioning factor is often used to analyze landslide susceptibility. It has an impact on the land's surface, changing the location of rainfall, vegetation, erosion, and soil depth (Pham et al., 2022). It also significantly affects soil moisture, slope gradient, stream, and drainage density.

Slope

Slope, which influences the shear forces operating on hill slopes, is typically regarded as one of the crucial factors for landslide modeling (Nolasco-Javier et al., 2015). The probability of landslides rises with steeper slope angles because these conditions promote runoff and drainage processes at the cost of soil stability. According to Magliulo et al. 2008, slope gradient considerably impacts groundwater flow and the concentration of soil moisture, which are directly connected to landslide occurrence.

Slope aspect

The slope's aspect or exposure indicates the direction in which it is oriented (Barman et al., 2023). Conditioning exposure to sunlight and drying winds that control soil moisture and evapotranspiration (Tang et al., 2020) is an indicative factor of landslide susceptibility. This factor can influence other factors, including wind direction, rainfall regime, amount of sunlight, hydrology, vegetation development, and soil moisture (Xing et al., 2021).

Curvature

The curvature is the change in the topographic surface's slope over a narrow curve arc, also called slope shape or topographic curvature. It influences the direction of surface flow and the constraint on the slope material.

Profile curvature

Profile curvature is the term used to describe the curvature in the primary direction of the steepest slope. This factor impacts how quickly and slowly the flow moves, impacting erosion and deposition (Xie et al., 2021). A positive or negative value denotes the cell is part of a concave or convex upward slope.

Plan curvature

The curvature of a plane is defined by the contour line created when the surface intersects a horizontal plane. It controls the water direction during downslope flow, which can condition landslide events (Habumugisha et al., 2022; Tavakkoli Piralilou et al., 2019). The cell is a portion of a laterally concave or convex slope, whether the value is positive or negative.

TPI

The Topographic Position Index (TPI) is a parameter to describe the terrain (Andrew D. Weiss, 2001). It refers to the difference in altitude between a point and its surroundings. It is the outcome of comparing each cell's height in a DEM to the average elevation of its surrounding cells. The TPI is positive for cells elevated above their surroundings (ridges and hilltops) and negative for depressions.

TWI

The water saturation zones and soil moisture content are represented by the Topographic Wetness Index (TWI). This factor was chosen because it explains how topography affects soil moisture. Higher values of TWI can be related to higher risks of landslides (Meena et al., 2022).

Lithology

Lithology is one of the most frequently employed parameters in landslide susceptibility studies due to its impact on the geo-mechanical properties of the terrain (Costanzo et al., 2012). The variation of lithological units often leads to differences in permeability, density, hardness, and strength of soils and rocks. The lithological map was created from various sources, including the United States Geological Survey's (USGS) geological data for Africa and the 1:200,000 geological map of Morocco. Eight lithological units were distinguished and assigned the following codes:

- Quaternary (marls, sandstone, limestone, and alluvium) = 0
- Lower Jurassic (limestone and molasses), Cretaceous (marls and marly limestone), and Cretaceous-Tertiary (marls, marly limestone, and flysch) = 1
- Tertiary (limestone and flysch) =2
- Lower Cretaceous (Flyschs), tertiary intrusive rock, tertiary intrusive rock, and Triassic (basalt) = 3.

Precipitation

Precipitation is one of the main initiators or triggers of landslide risk. It raises pore pressure and water content of the soil, reducing soil cohesion and potentially leading to slope instability and mass movement (Habumugisha et al., 2022). The calculation of monthly average precipitation spanning 16 years (2005–2021) was performed using data from the Climate Hazards Group InfraRed Precipitation with Stations (CHIRPS) (Funk et al., 2015). The CHIRPS data were preferred because several studies concluded that CHIRPS performs better than TRMM 3B42 (Tropical Rainfall Measuring Mission version 7) and PERSIANN-CCS (Precipitation Estimation from Remotely Sensed Information using Artificial Neural Networks – Cloud Classification System) (Karmouda et al., 2022). For the past 16 years, the research region has received an average of 35.19 to 68.50 mm of rain each month.

Land cover/ land use

The physical characteristics of soils, as well as the hydrological processes of rainfall distribution, infiltration, slopes, and runoff, may all be influenced by land use (Meena et al., 2022). These data for 2021 in our study area were directly extracted from ESRI's annual 10m land cover maps, derived from ESA's Sentinel-2 imagery at 10m resolution. These were produced by the Impact Observatory, which employed a deep-learning model trained for land classification using billions of human-labeled pixels. The methodology for encoding the land cover parameters was as follows: Water = 1, Built area = 2, Bare ground = 3, Range Land = 4, Flooded vegetation = 5, Crops = 6, and Trees = 7.

Distance to roads

One of the human factors that could promote various forms of erosion is the distance to roads, especially the occurrence of landslides. Road construction requires excavation and dumping of material, which impacts slope stability, and vibrations generated by human activities can trigger mass movements (Vakhshoori & Zare, 2016). The road distance calculation was derived from the road network extracted from Google Earth through a GIS tool.

NDVI

The presence and type of vegetation cover are essential to mass movement, influencing slope stability by water absorption and reinforcing soil cover (Xing et al., 2021). A high (NDVI) value may also suggest an elevated likelihood of such events (Huang et al., 2020). Vegetation density was obtained by calculating the Normalized Difference Vegetation Index (NDVI) on Google Earth Engine (GEE), using a one-year time series (January to December 2021) derived from cloud-free images of the Sentinel-2A and Sentinel-2B satellites. The NDVI map was calculated according to Equation 1:

$$NDVI = \frac{NIR - RED}{NIR + RED} \tag{1}$$

NIR and RED refer to the spectral reflectance measurements obtained within the red and near-infrared bands of the electromagnetic spectrum, respectively. The NDVI value varies within the range of -1 to 1.

Distance to faults

The distance from a fault is a significant geological factor that can potentially trigger landslides, and it has been utilized in numerous prior studies related to landslide susceptibility (Habumugisha et al., 2022). Areas near geological faults are at high risk for landslides because the surrounding rock experiences significant fracturing, decreasing its strength due to tectonic fractures (Chen et al., 2017).

Distance to rivers

Many landslides are caused by rivers because of their power to erode exposed material, thus becoming a key factor in landslide susceptibility (Pradhan et al., 2010). This factor was computed using the "Euclidean Distance" from the drainage network derived from the SRTM DEM data and refined using Google Earth for improved accuracy.

Modeling using Machine Learning Algorithms

Multivariate discriminant analysis

Multivariate discriminant analysis (MDA) is a multivariate statistical method that complements linear discriminant analysis (LDA). It performs a mixture of classifiers for clustering by merging the implementation of simple linear and non-linear combination models. The MDA algorithm has many advantages, including its ability to handle large and high-dimensional datasets, avoid overfitting of datasets, and be easy to use (Hastie & Tibshirani, 1996). It is a widely employed supervised machine learning methodology utilized for both regression and classification tasks in various fields, including natural resources modeling and landslide susceptibility assessments (Kalantar et al., 2019).

Logistic regression

Logistic regression (LR) is a simple, rapid, and highly efficient classification method (Rajaneesh et al., 2022). It is one of the most commonly utilized machine learning algorithms, originally developed within the statistical field (Cabrera, 1994). The generalization of the linear model relies on employing the logistic function to represent a binary response variable (dependent variable, landslide occurrence) and numerous explanatory variables (independent variables, conditioning factors) to predict the likelihood of specific events, such as landslides (Xie et al., 2021).

The classification output is between 0 and 1, making it applicable for probabilistic interpretation in several study areas (Qu et al., 2019).

Classification and regression Ttees

Classification and regression trees (CART), introduced by Breiman in 1984, represent predictive algorithms employed in the machine learning field. Instead of using stopping rules, CART grows an extensive tree to produce a sequence of subtrees for solving classification problems (Loh, 2011). The decision tree algorithm has been demonstrated to be highly effective in dealing with classification. It has the noticeable advantage of handling small datasets and scaling to significant problems (Markham et al., 2000). The model is a non-parametric procedure for predicting output variables using input variables (Prakash, 2018). CART has found extensive application in landslide studies across various global regions (Felicísimo et al., 2013; Rabby & Li, 2020; Vorpahl et al., 2012), although, to the best of our knowledge, it has not been applied in Morocco. In the context of landslide prediction, the CART algorithm undergoes a four-step training process: (i) tree construction, (ii) determination of tree construction termination, (iii) tree pruning, and (iv) selection of the optimal tree for classifying landslide and non-landslide categories (Loh, 2011).

Support Vector Machine

Support Vector Machine (SVM) is an efficient and robust supervised technique applicable for both regression and classification tasks. (Cortes & Vapnik, 1995; Cristianini & Shawe-Taylor, 2000). The most crucial feature of SVM is its kernel function, which transforms the input variables into a complex and multi-dimensional linear space through nonlinear transformation. This generates an optimal separation hyperplane between two classes (Qu et al., 2019) to maximize the margin between them, thereby making it a nonlinear classifier. There are typically four categories of Kernel functions utilized in SVM: linear, sigmoid, radial basis, and polynomial functions. In this study, the linear function was chosen for the SVM model to compute the landslide susceptibility index. SVM classification has demonstrated its effectiveness in landslide susceptibility mapping, outperforming various other machine learning methods (Xie et al., 2021), especially in mountainous areas.

Model validation and performance

As landslide mapping involves binary classification (absence or presence of landslides), it is crucial to assess the quality of landslide probability estimates. This assessment should consider prediction accuracy, misclassification errors, and outcomes (Merghadi et al., 2020). Before model validation, the dataset must be divided into training and testing parts. Previous studies have commonly used simple random division (Kadavi et al., 2018). Nevertheless, we chose to employ robust statistical validation through k-fold cross-validation to address the issue of imbalanced landslide samples and mitigate bias (Pal & Patel, 2020). Using this approach, the dataset is divided randomly into 10 subsets or folds, with each fold employed to validate the model trained on the remaining folds. This hold-out process is repeated 10 times. The evaluation is intended to identify and compare the accuracy of the four machine learning models across the Taounate province. The landslide susceptibility values of the four models, which ranged from 0 to 1, were compared with the landslide feature based on two predicted landslide classes: "positive" if the value was more significant than 0.5 and "negative" if the value was less than 0.5. From these values, six statistical measures were calculated, including precision, sensitivity (recall), specificity, accuracy, F1-measure (or F1-score), and receiver operating characteristics (ROC), as follows:

$$Sensitivity = \frac{TP}{TP + FN} \tag{2}$$

$$Specifictity = \frac{TN}{TN + FP} \tag{3}$$

$$Accuracy = \frac{TN + TP}{TN + TP + FN + FP} \tag{4}$$

$$Precision = \frac{TP}{TN + FP} \tag{5}$$

$$F1 - measure = \frac{2 \times TP}{2 \times TP + FN + FP} \tag{6}$$

where: "P" represents the total number of landslides, "N" represents the number of non-landslide points, "True Positives (TP)" and "True Negatives (TN)" denote correctly classified samples, and "False Positives (FP)" and "False Negatives (FN)" represent misclassified samples.

The ROC curve, as introduced by Bradley, 1997, is a commonly used method for assessing the predictive capabilities of a model. The area under the ROC curve (AUC) serves as a performance metric that considers specificity on the x-axis and sensitivity on the y-axis (Jiang et al., 2023). AUC values are between 0 and 1 and can be classified as excellent (0.9–1), very good (0.8–0.9), good (0.7–0.8), average (0.6–0.7) and poor (0.5–0.6). According to Mathew et al., 2009, the AUC is a noteworthy metric and one of the most valuable precision statistics for landslide susceptibility analysis.

Factor importance

For geo-environmental models, it is necessary to determine which factors are essential or contribute the most to the disaster. There is no universal guide for identifying these factors, and several methods have been proposed in recent years. We opted for a jack-knife test based on removing one factor at a time and using the remaining factors for modeling (Lombardo et al., 2016; Ramos-Bernal et al., 2019). The jack-knife test is employed to ascertain the individual contributions of each factor to the overall susceptibility model (Ramos-Bernal et al., 2019). The sensitivity of each of the fifteen factors in each predictive model has been assessed using the percentage decrease in overall accuracy (DAAC) (Bouramtane et al., 2022).

$$DACCi = \frac{ACC_{all} - ACC_{i}}{ACC_{all}} \times 100 \tag{7}$$

ACC_{all} represents the calculated model accuracy when all parameters are considered. ACC_i denotes the accuracy value of the model when an indicator 'i' is excluded from the input data, and $DACC_i$ represents the corresponding percentage decrease in accuracy.

RESULTS

Comparative performance analysis of machine learning models

According to the AUC index, the variation in model performance was minimal. All four models performed excellently for landslide predictive ability with AUC values above 0.95. The CART model achieved the highest score (AUC=0.971), followed by LR (AUC=0.963), with SVM (AUC=0.961) and MDA (0.954) following suit (Figure 4). Evaluating model performance relying only on one assessment measure, such as AUC, might not be suitable, as a high AUC value does not invariably signify elevated accuracy in spatial prediction (Kalantar et al., 2019). Therefore, five statistical measures were used: precision, sensitivity, specificity, accuracy, and F1-measure. All the results are presented in Table 2. The SVM model exhibited superior performance in classifying both landslide and non-landslide in both the training and test datasets,

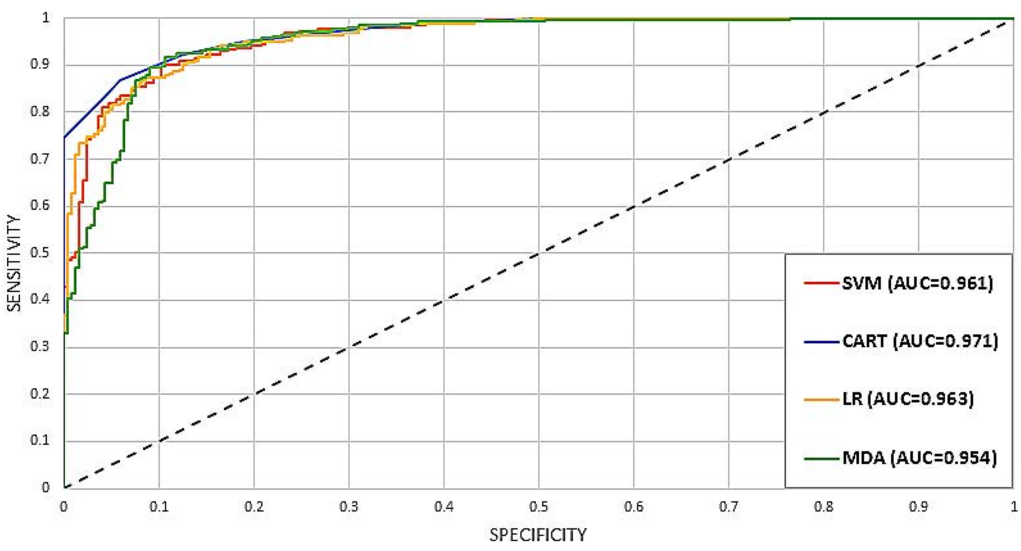

Figure 4. The area under curve (AUC) related to the five employed models: support vector machine (SVM), classification and regression trees (CART), logistic regression (LR) and multivariate discriminant analysis (MDA)

Table 2. The performance of four models in terms of evaluation measures

Measures	MDA		LR		SVM		CART	
	Training	Test	Training	Test	Training	Test	Training	Test
Precision	93.07%	70.12%	90.15%	81.62%	89.89%	81.74%	87.59%	71.43%
Specificity	93.92%	61.77%	90.36%	78.06%	89.97%	79.46%	87.42%	65.82%
Sensitivity	82.56%	91.60%	89.16%	90.29%	89.94%	89.24%	90.24%	77.69%
Accuracy	88.24%	75.95%	89.69%	83.01%	89.92%	83.01%	89.10%	69.02%
F1-measure	77.79%	60.84%	81.24%	79.12%	81.66%	72.48%	80%	54.67%

achieving accuracies of 89.92% and 83.01%, respectively. The LR model came in second with an accuracy of 89.69% and 83.01% for both the training and test datasets, subsequently followed by the CART with 88.1% for the training dataset and 69.02% for the test dataset. Finally, the MDA model achieved accuracies of 88.24% for the training dataset and 75.95% for the test dataset. Moreover, the SVM model also showed superior performance in terms of precision and specificity (non-landslide classification) for the test data, with 81.74% and 79.46%, respectively. However, the best performance of the training data for precision and specificity was attained by the MDA model (93.07%, 93.92%), which is followed by the LR model (90.15%, 90,36%), which is then followed by the SVM model (89.89%, 89.97%) and CART model (87.59%, 87.42%). The CART model achieved the highest sensitivity for the training dataset at 90.24%, whereas the LR model demonstrated the highest sensitivity for the test dataset at 91.60%. Furthermore, the LR model exhibited superior performance regard to the F1-measure for both the training dataset (81.69%) and the test dataset (79.12%). It is crucial to highlight that the outcomes of our research study do not necessarily imply that the SVM model is the optimal machine learning approach for every prediction or classification assignment. However, our findings demonstrate that the SVM model outperformed the other methods in several classification tasks, especially the accuracy, indicating its potential as a suitable option for landslide susceptibility mapping not only in the Rif region but also in other similar contexts.

Landslide susceptibility maps

Figure 5 illustrates the landslide susceptibility maps. The use of the four models resulted in a consistent distribution of susceptibility prediction categories, with high susceptibility areas primarily concentrated in the northern and northwestern regions of the study area. Conversely, regions characterized by low susceptibility were situated in the southern part. Meanwhile, areas displaying varying degrees of susceptibility, ranging from high to moderate, were observed in the central, east-central, and west-central regions of the study area. Subsequently, the relative proportions of the four classes in each model were computed (Figure 6). The proportion of the very high susceptible area was comparable between the CART and SVM models, constituting 42% in both cases, slightly higher for the LR model (45%) and lower for the MDA model (40%). On the other hand, the differences between the models were stronger for the low susceptibility category, ranging from 28% for the CART model to 37% for the MDA model. For the medium and high susceptibility categories, there were some similarities between the four models, as they occupy less than 16%.

Contribution of conditioning factors to landslide distribution

Figure 7 illustrates the explanatory variables' contribution for each model and is represented by the number of observations appearing on the x-axis. Precipitation had very high DAAC values ranging from 6.52% to 14.66%. From this finding, it is concluded that precipitation is the most crucial factor that significantly affects the distribution of landslides for each classifier in the research region, followed by distance to the rivers with DAAC values ranging from 4.21% to 3.04%. However, it appears that distance to roads and land cover/land use held relatively lower significance within the study area, as indicated by the outcomes of the four classifiers. The comparative importance of precipitation, distance to rivers, land cover, and

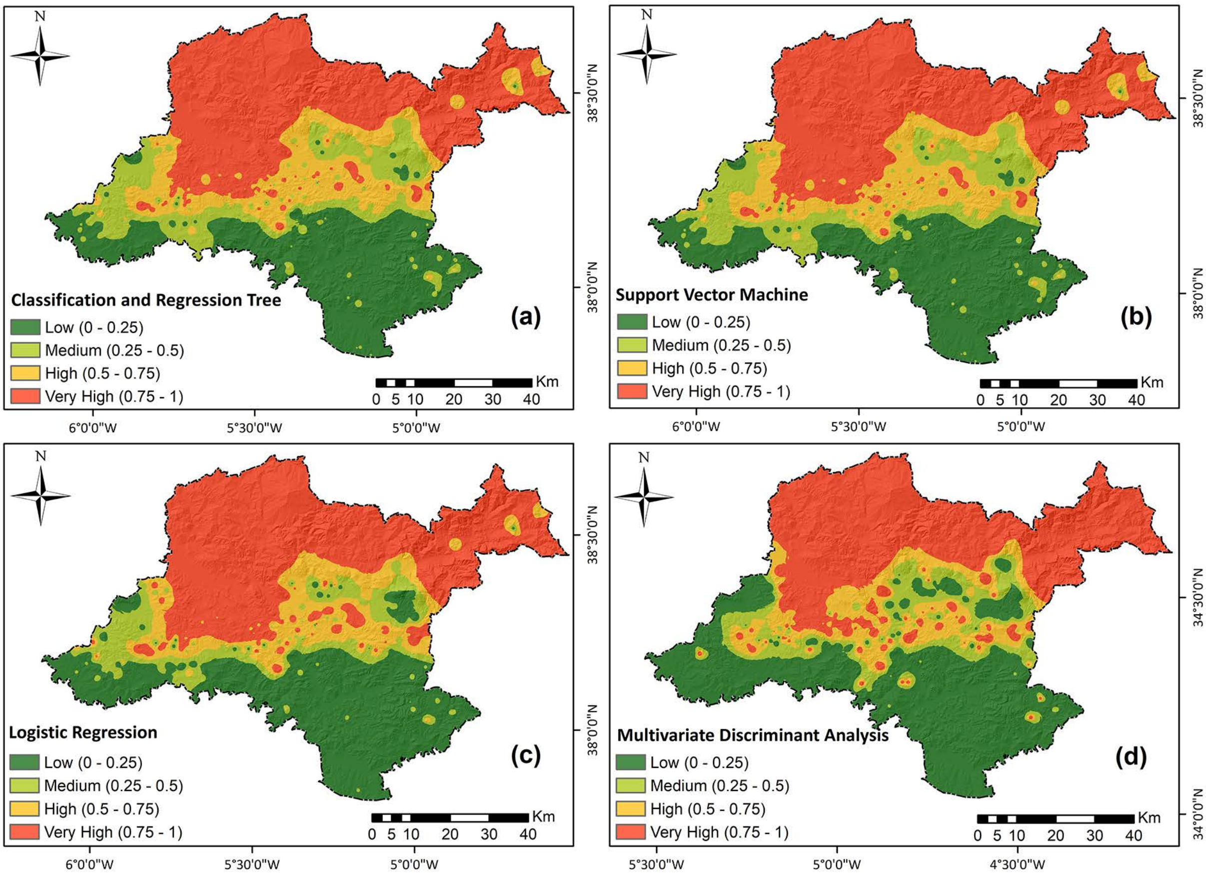

Figure 5. Landslide susceptibility maps of Taounate province using the four models (a) CART, (b) SVM, (c) LR and (d) MDA

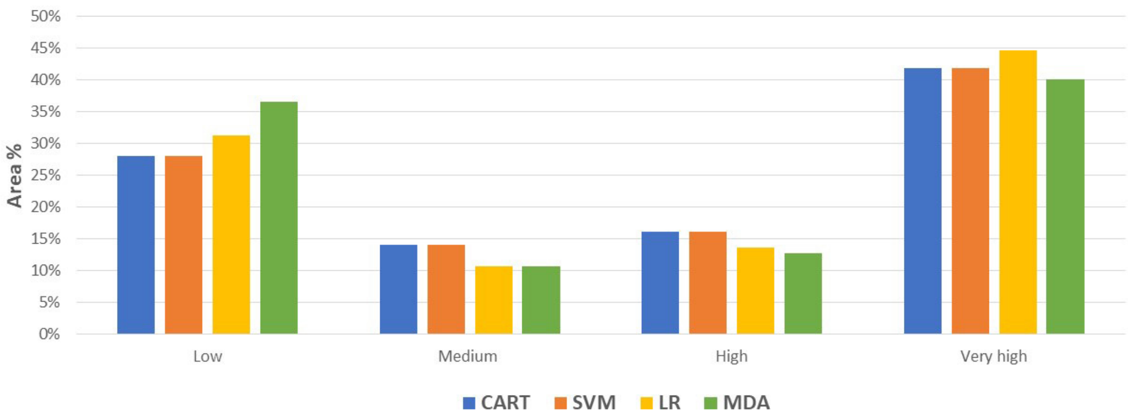

Figure 6. The percentages of areas occupied by four susceptibility levels (low, medium, high, very high)

distance to roads was similar among the four models. However, the relative importance of the remaining conditioning factors varied significantly across the models. Notably, the SVM model attributed the highest DAAC value to precipitation (14.66%), marking it as the most influential factor. It was followed by slope (5.25%), distance to rivers (4.16%), altitude (2.84%), and distance to faults (2.84%).

DISCUSSION

Factors contributing to landslide risk in the Rif region

The investigation into landslide susceptibility is essential in land management, planning, and the development of hilly regions. These susceptibility maps are valuable tools for government agencies, offering essential guidance for

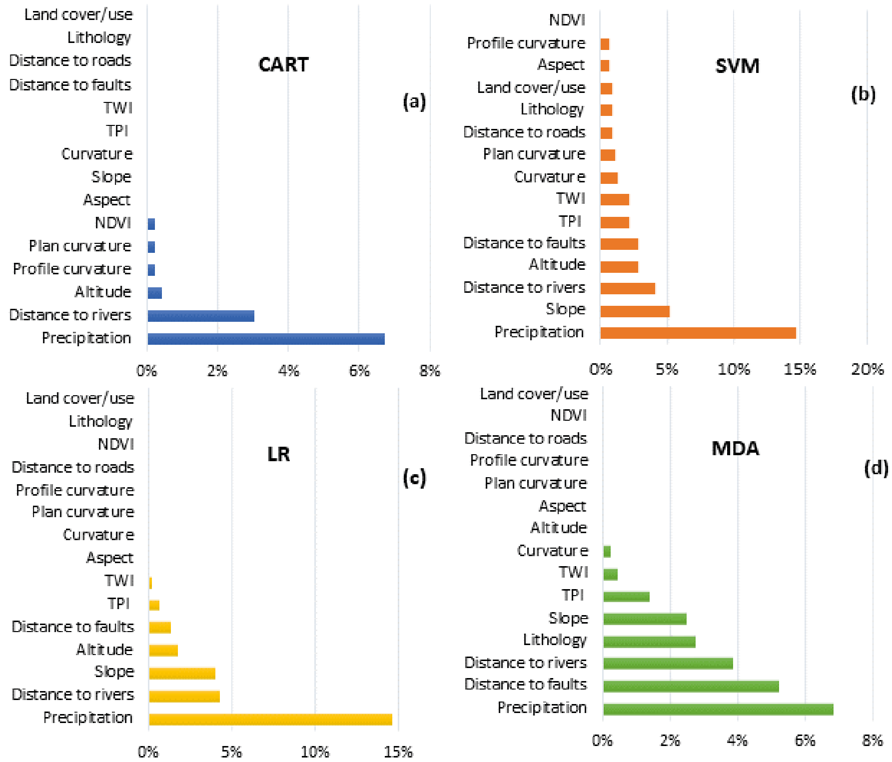

Figure 7. The contribution of the explanatory variables using DAAC for (a) CART, (b) SVM, (c) (LR) and (d) MDA models

effective decision-making in landslide hazard and risk analysis, as well as for general planning and assessment of landslides (Roccati et al., 2019). This study is innovative as it marks the initial endeavor to produce a comprehensive landslide susceptibility map encompassing the entire study region. The results revealed that nearly half, approximately 40% to 45%, of the study area exhibits a high susceptibility to landslides, as confirmed by the four machine learning models (Figure 6). Furthermore, the four susceptibility maps generated by machine learning show a uniform distribution of the different susceptibility levels, highlighting the study area's north-northeast regions as the most susceptible to landslides. Concurrently, the southern region is characterized as having a low susceptibility to landslides (Figure 5). The region exhibiting a notably elevated susceptibility to landslides is characterized by high precipitation, particularly in the north, along with contrasting relief. Flat and gentle slopes identify the low susceptible as gentle slopes. In summary, the landslide susceptibility maps produced in this study offer valuable resources for urban planners, government entities, and non-governmental organizations. These maps can aid in the effective management of human activities, resources, and infrastructure development within the region. The increased human activities in the region, combined with the landslide susceptibility maps generated, have the potential to enable local authorities to precisely identify areas at high risk and put in place early warning and preventive strategies for disaster mitigation.

Recent studies have noted a continuous increase in the frequency of extreme precipitation events in Mediterranean regions (Fiori et al., 2014; Tramblay & Somot, 2018), translating into the more frequent occurrence of natural hazards, especially landslides and floods. The dominance of precipitation (DAAC between 16.72 and 14.66) over other factors in mapping landslide-prone areas was expected since precipitation is regarded as the primary triggering factor for landslide movement and degradation, particularly in mountainous terrains (Argyriou et al., 2022; D'Ippolito et al., 2023; Tsunetaka, 2021). These results and findings are in line with the climatic characteristics of the study area, which includes both the Rifian region and the wider Mediterranean region. These areas are distinguished by substantial rainfall during the wet season (from November to February) and during summer, often in the form of storms (Senoussi et al., 1999).

Moreover, several studies have indicated that the effect of climate change through severe drought during the year, followed by aggressive precipitation, affects the stability of slopes at different temporal and geographical scales, triggering landslides (Stoffel et al., 2014). Precipitation reduces friction between substances and increases the pressure of water in soil pores, thus increasing the risk of breakage (Earth Science Data Systems, 2020). The impact of rainy events on landslide triggers in the Rif region has been documented by El Kharim et al., 2021. Their landslide inventory in Chefchaouen, located west of our study area, established a strong correlation between soil movement and rainfall. Furthermore, they observed that the fastest soil movement coincides with the rainiest months, specifically January and February. During these months, the layers constituting the core of both old and recent landslides experience accelerated gravitational deformation compared to other periods of the year.

In nearly all machine learning models, after precipitation, the secondary factors influencing landslide susceptibility mapping include slope, distance to rivers, elevation, and distance faults (Figure 7). These four factors are associated with the geo-morphology characteristics of the study area, as the Rif region is known for its rugged topography, rough relief, and steep slopes. Geologically, it is a seismically active area with active regional faults and large shearing areas (Poujol et al., 2014). Such conditions made the drainage network flow mainly on fault corridors, deep valleys with steep slopes, following their orientation and adopting their structuring, leading to the formation of several types and patterns of drainage, especially trellis, rectangular, and barbed network patterns, which reflect an intense structural geological control on the drainage network (Bouramtane et al., 2020). As a result, the development of landslides frequently begins with the incision of rivers along the main faults and valleys, which defines the rhythm of the landscape's evolution. The slopes of the hills then respond to this incision by destabilizing the slopes' base and increasing the moisture content of the soil, leading to landslides, and risk is thus concentrated at the drainage networks (Figure 8) (Clapuyt et al., 2019). Furthermore, this frequently observed spatial proximity of landslides to drainage networks is known as connectivity; it is crucial for large landslides in high-relief areas, and it is one of the distributional characteristics of landslides that determine their role as a natural hazard (Li et al., 2016; Roback et al., 2018).

The incorporation of the "distance to faults" factor among the prominent variables implies an

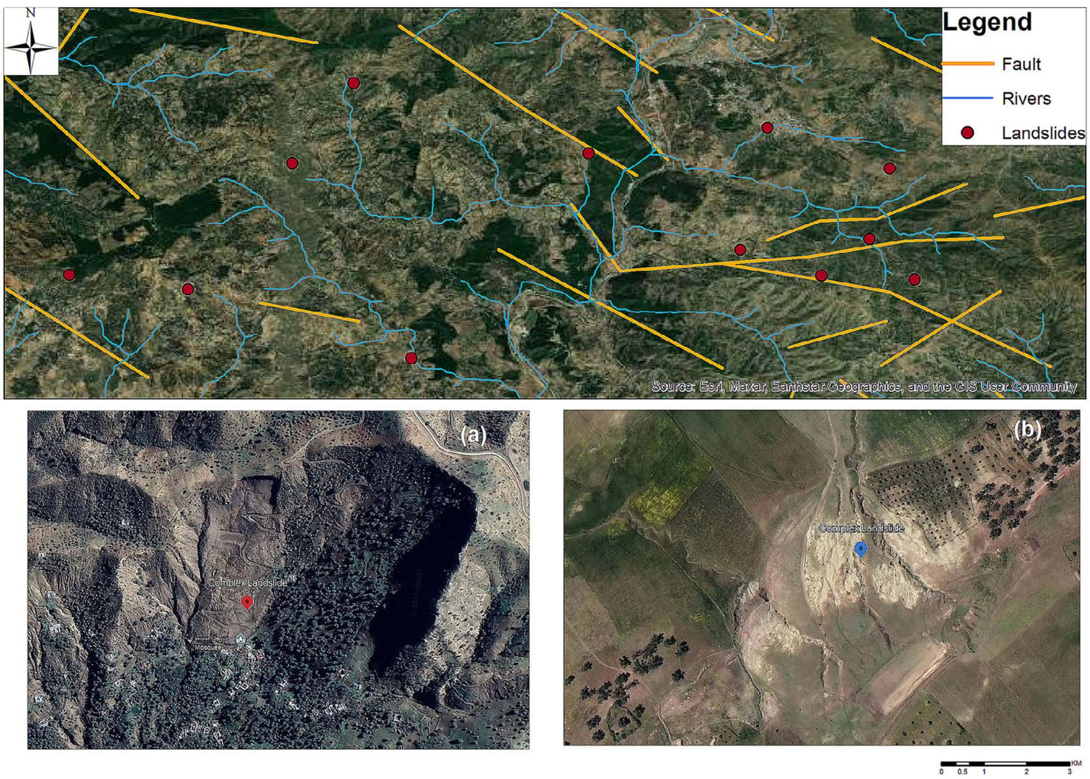

Figure 8. A map displaying landslides near faults and rivers: (a) near a fault and (b) near a stream

association with the landslides identified in the study area, particularly those situated in close proximity to the major faults within the study area (Figure 8). This indicates the influence of tectonic activity on landslide risk, particularly the occurrence of co-seismic landslides. These co-seismic landslides are a significant secondary natural hazard in earthquake-prone mountainous regions, such as the Rif structural zone (Hovius et al., 2011; Roback et al., 2018). Indeed, the Rif structural zone, particularly its eastern part covering the province of Taounate, experienced its last major earthquake of Mw 6.4 in 2004 and its most recent Mw 5.2 earthquake on 07/01/2023, with several Mw 4 to 4.9 earthquakes occurring throughout 2022. However, no studies have been conducted to date that directly link the study area's seismic activity to the occurrence of its landslides.

Performance evaluation of machine learning models for landslide susceptibility mapping

Several statistical methodologies have been recently employed to model landslide susceptibility in some limited areas of Taounate province in the Rif Mountains, including Ain aicha, Ourha, Oudka, and Taounate City. However, compared to conventional statistical analysis, machine learning methods demonstrate enhanced efficiency in addressing real-world challenges, such as landslide occurrences (B. Zhao et al., 2022). Machine learning methods have become increasingly valuable tools for decision-makers as they facilitate the identification of relationships between geological, topographical, climatic factors, human activities, and landslide events. Hence, comparative studies are needed to evaluate the performance of the models under the same conditions and make a fair judgment about their capabilities (Rahmati et al., 2019). In this present study, four machine learning models, namely SVM, CART, LR, and MDA, were compared and evaluated to map landslide susceptibility and identify the most significant causative factors. All four machine learning methods demonstrated excellent performance, highlighting the robust capabilities of machine learning modeling in the study area, with AUC scores ranging from 0.954 to 0.971 (Figure 4). The CART model demonstrated superior performance with an AUC value of 0.971. However, based on the evaluation metrics such as accuracy (89.92%, 83.01%), precision (81.74%), specificity (79.46%), and F1-measure (81.66), the SVM model performs at the highest level (Table 2). SVM is, therefore, the most appropriate choice for mapping landslide susceptibility in mountainous regions. In this present study, our results align with earlier research conducted by Naceur et al., 2022, who employed models like Weight of Evidence (WoE), Radial Basis Function Network (RBFN), and SVM in the high Atlas of Morocco; Yousefi et al., 2020, conducted research in a mountainous region in Iran, utilizing Generalized Linear Model (GLM); Functional Discriminant Analysis (FDA) and SVM; Pham et al., 2016, who applied Naïve Bayes (NB), Bayesian Network (BN), Naïve Bayes (NB), LR, SVM and Fisher's Linear Discriminant Analysis (FLDA) in India; Xie et al., 2021 conducted a study in China to assess landslide susceptibility using various methods, including SVM, and subsequently compared their performance. The SVM model achieved greater predictive accuracy due to its reliance on minimizing structural risk over traditional empirical risk minimization, aiming for a globally optimal solution for solving complex nonlinear problems (C. Zhou et al., 2018). It is suitable for predicting high-dimensional data, can also work on small data sets, and is robust when dealing with slight sample variations (Youssef & Pourghasemi, 2021). However, SVM is not an interpretable model, and it consumes much memory and time compared to other models (Marjanović et al., 2011).

The CART model exhibited superior performance compared to all other models, as shown by the AUC and sensitivity indexes (AUC=0.971; sensitivity= 90.24%). This can be attributed to the capability of decision tree models to effectively address nonlinear problems and work on high-dimensional data accurately (Razi & Athappilly, 2005). However, decision trees tend to overfit and do not generalize well to new data, and a slight change in the data can produce a very different decision tree (Hong, 2023). The results do not necessarily indicate that LR and MDA have the lowest predictive ability since they demonstrated high accuracy in AUC and some classification tasks. LR performed the best in terms of the F1-measure index and the second-highest AUC rate of 0.963. However, MDA performed best in terms of accuracy and specificity of training data (93.07%, 93.92%), as well as the sensitivity of test data (91.6%), which is considered a very good result for a linear model (Figure 4, Table 2). Moreover, the advantage of using the nonparametric MDA algorithm lies in its ability to perform effectively in the presence of complex associations (Pourghasemi et al., 2021). The LR and MDA models are sensitive to linear correlation of influencing factors, which are not adept at modeling complex nonlinear problems (C. Zhou et al., 2018). However, the fact that the LR and MDA results are highly satisfactory and comparable to those of the SVM and CART models suggests the presence of a likely linear correlation between landslide occurrence and geo-environmental factors, which are likely the primary drivers of the landslide issue in the study region. Furthermore, using LR or MDA has a significant advantage in efficiently interpreting their findings. This is due to the standardized coefficients generated (Figure 9) by the LR model and the correlation factors (Figure 10) identified by the MDA model, which allows the identification of the processes that condition natural hazards through their interpretation of the LR model.

CONCLUSIONS

Identifying robust and efficient models to reduce errors in landslide susceptibility modeling and delimitation of landslide-prone areas is essential. The primary objective of this study is to evaluate four machine learning models (SVM, CART, LR, and MDA) for the purpose of mapping landslide-prone regions and gaining insights into the geo-environmental processes governing landslides in one of the most impacted areas in North Africa. 255 landslides were identified and collected with 15 landslide conditioning factors to develop the four machine-learning models. The dataset was divided into ten random divisions: 30% of the dataset was allocated for testing, while 70% was reserved for training. Six statistical measures, namely accuracy, precision, sensitivity (recall), specificity, F1-measure (or F1-score), and receiver operating characteristics (ROC), were used to compare the four models. The findings of the causal significance analysis indicate that landslides are primarily triggered by rainfall. Most of these occurrences are observed on slopes near rivers and faults, highlighting the significant influence of precipitation on landslides in the Rif mountains. The comparison results demonstrate that all four models have excellent and relatively

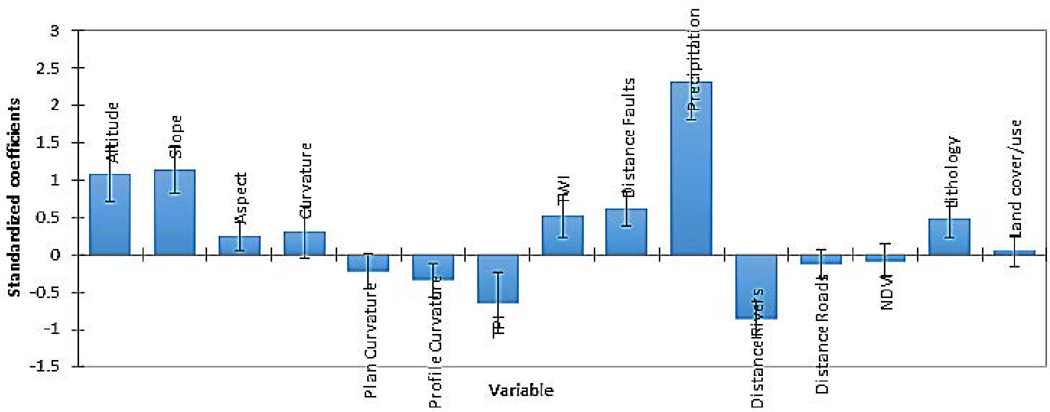

Figure 9. Standardized logistic regression coefficients of LR model

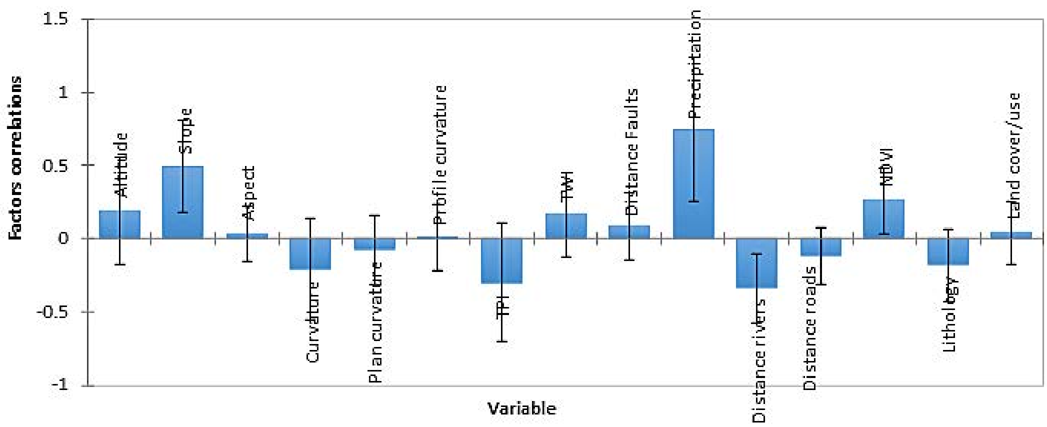

Figure 10. Factors correlation of MDA model

similar performance (ROC curve > 0.954), but the SVM model performs best. The SVM model achieved the highest accuracy and F1-measure for the training data and the highest accuracy, precision, and specificity for the test data. Although the prediction accuracy of LR and MDA models is not as high as that of SVM, they outperformed the other models in some tasks and offer the advantage of providing more interpretable results regarding landslide hazard conditioning processes. Areas with a very high susceptibility to landslides make up nearly half of the study area, ranging from 40% to 45%. These areas are situated in the north and northwest, characterized by heavy precipitation and high relief. All four landslide models demonstrated strong performance in landslide susceptibility assessment, with the SVM model standing out as the top performer. Consequently, it is recommended for use in the creation of improved landslide susceptibility maps to enhance landslide hazard management. This study offers valuable insights for decision-makers in devising disaster risk reduction strategies in North Africa, particularly in regions sharing similar geo-environmental and climatic conditions. For future studies, it is essential to account for the distinct characteristics and influential factors specific to each type of landslide when crafting predictive models for their occurrence. Additionally, the combination of SVM with LR or MDA holds the potential to enhance model performance and offer a more comprehensible interpretation of landslide mechanisms.

REFERENCES

1. Abdı, A., Bouamrane, A., Karech, T., Dahri, N., & Kaouachi, A. (2021). Landslide Susceptibility Mapping Using GIS-based Fuzzy Logic and the Analytical Hierarchical Processes Approach: A Case Study in Constantine (North-East Algeria). Geotechnical and Geological Engineering, 39(8), 5675–5691. https://doi.org/10.1007/s10706-021-01855-3
2. Abidi, A., Demehati, A., & El Qandil, M. (2019). Landslide Susceptibility Assessment Using Evidence Belief Function and Frequency Ratio Models in Taounate city (North of Morocco). Geotechnical and Geological Engineering, 37(6), 5457–5471. https://doi.org/10.1007/s10706-019-00992-0
3. Ado, M., Amitab, K., Maji, A. K., Jasińska, E., Gono, R., Leonowicz, Z., & Jasiński, M. (2022). Landslide Susceptibility Mapping Using Machine Learning: A Literature Survey. Remote Sensing, 14(13), Article 13. https://doi.org/10.3390/rs14133029
4. Anis, Z., Wissem, G., Vali, V., Smida, H., & Essghaier, G. M. (2019). GIS-based landslide susceptibility mapping using bivariate statistical methods in North-western Tunisia. Open Geosciences, 11(1), 708–726. https://doi.org/10.1515/geo-2019-0056
5. Argyriou, A. V., Polykretis, C., Teeuw, R. M., & Papadopoulos, N. (2022). Geoinformatic Analysis of Rainfall-Triggered Landslides in Crete (Greece) Based on Spatial Detection and Hazard Mapping. Sustainability, 14(7), Article 7. https://doi.org/10.3390/su14073956
6. Barman, J., Ali, S. S., Biswas, B., & Das, J. (2023). Application of index of entropy and Geospatial techniques for landslide prediction in Lunglei district, Mizoram, India. Natural Hazards Research. https://doi.org/10.1016/j.nhres.2023.06.006
7. Benabdelouahab, T., Gadouali, F., Boudhar, A., Lebrini, Y., Hadria, R., & Salhi, A. (2020). Analysis and trends of rainfall amounts and extreme events in the Western Mediterranean region. Theoretical and Applied Climatology, 141(1), 309–320. https://doi.org/10.1007/s00704-020-03205-4
8. Benchelha, S., Aoudjehane, H. C., Hakdaoui, M., El Hamdouni, R., Mansouri, H., Benchelha, T., Layelmam, M., & Alaoui, M. (2020). Landslide Susceptibility Mapping in the Commune of Oudka, Taounate Province, North Morocco: A Comparative Analysis of Logistic Regression, Multivariate Adaptive Regression Spline, and Artificial Neural Network Models. Environmental & Engineering Geoscience, 26(2), 185–200. https://doi.org/10.2113/EEG-2243
9. Bouramtane, T., Hilal, H., Rezende-Filho, A. T., Bouramtane, K., Barbiero, L., Abraham, S., Valles, V., Kacimi, I., Sanhaji, H., Torres-Rondon, L., de Castro, D. D., Vieira Santos, J. da C., Ouardi, J., Beqqali, O. E., Kassou, N., & Morarech, M. (2022). Mapping Gully Erosion Variability and Susceptibility Using Remote Sensing, Multivariate Statistical Analysis, and Machine Learning in South Mato Grosso, Brazil. Geosciences, 12(6), 235. https://doi.org/10.3390/geosciences12060235
10. Bouramtane, T., Tiouiouine, A., Kacimi, I., Valles, V., Talih, A., Kassou, N., Ouardi, J., Saidi, A., Morarech, M., Yameogo, S., Kbiri, H. E., Rhazal, H., Achach, H., & Barbiero, L. (2020). Drainage Network Patterns Determinism: A Comparison in Arid, Semi-Arid and Semi-Humid Area of Morocco Using Multifactorial Approach. Hydrology, 7(4), Article 4. https://doi.org/10.3390/hydrology7040087
11. Brahim, L. A., Bousta, M., Jemmah, I. A., Hamdouni, I. E., ElMahsani, A., Abdelouafi, A., Alaoui, F. S., & Lallout, I. (2018). Landslide susceptibility mapping using AHP method and GIS in the peninsula of Tangier (Rif-northern morocco). MATEC Web of Conferences, 149, 02084. https://doi.org/10.1051/matecconf/201814902084

12. Bravo-López, E., Fernández Del Castillo, T., Sellers, C., & Delgado-García, J. (2022). Landslide Susceptibility Mapping of Landslides with Artificial Neural Networks: Multi-Approach Analysis of Backpropagation Algorithm Applying the Neuralnet Package in Cuenca, Ecuador. Remote Sensing, 14(14), Article 14. https://doi.org/10.3390/rs14143495
13. Broeckx, J., Vanmaercke, M., Duchateau, R., & Poesen, J. (2018). A data-based landslide susceptibility map of Africa. Earth-Science Reviews, 185, 102–121. https://doi.org/10.1016/j.earscirev.2018.05.002
14. Chen, W., Pourghasemi, H. R., Kornejady, A., & Zhang, N. (2017). Landslide spatial modeling: Introducing new ensembles of ANN, MaxEnt, and SVM machine learning techniques. Geoderma, 305, 314–327. https://doi.org/10.1016/j.geoderma.2017.06.020
15. Chen, W., Shahabi, H., Zhang, S., Khosravi, K., Shirzadi, A., Chapi, K., Pham, B. T., Zhang, T., Zhang, L., Chai, H., Ma, J., Chen, Y., Wang, X., Li, R., & Ahmad, B. B. (2018). Landslide Susceptibility Modeling Based on GIS and Novel Bagging-Based Kernel Logistic Regression. Applied Sciences, 8(12), Article 12. https://doi.org/10.3390/app8122540
16. Clapuyt, F., Vanacker, V., Christl, M., Van Oost, K., & Schlunegger, F. (2019). Spatio-temporal dynamics of sediment transfer systems in landslide-prone Alpine catchments. Solid Earth, 10(5), 1489–1503. https://doi.org/10.5194/se-10-1489-2019
17. Earth Science Data Systems, N. (2020, August 19). Landslides Data Pathfinder [Data Pathfinder]. Earthdata; Earth Science Data Systems, NASA. https://www.earthdata.nasa.gov/learn/pathfinders/disasters/landslides-data-pathfinder
18. El Kharim, Y., Bounab, A., Ilias, O., Hilali, F., & Ahniche, M. (2021). Landslides in the urban and suburban perimeter of Chefchaouen (Rif, Northern Morocco): Inventory and case study. Natural Hazards, 107(1), 355–373. https://doi.org/10.1007/s11069-021-04586-z
19. El-Assri, E., Barnossi, A. E., Chebaibi, M., Hmamou, A., Asmi, H. E., Bouia, A., & Eloutassi, N. (2021). Ethnobotanical survey of medicinal and aromatic plants in Taounate, Pre-Rif of Morocco. Ethnobotany Research and Applications, 22, 1–23. Retrieved from https://ethnobotanyjournal.org/index.php/era/article/view/3113
20. El-Fengour, A., Motaki, H. E., & Bouzidi, A. E. (2021). Landslides susceptibility modelling using Multivariate Logistic Regression Model in the Sahla Watershed in Northern Morocco. Sociedade & Natureza, 33. https://doi.org/10.14393/SN-v33-2021-59124
21. Elmoulat, M., & Ait Brahim, L. (2018). Landslides susceptibility mapping using GIS and weights of evidence model in Tetouan-Ras-Mazari area (Northern Morocco). Geomatics, Natural Hazards and Risk, 9(1), 1306–1325. https://doi.org/10.1080/19475705.2018.1505666
22. Es-smairi, A., El Moutchou, B., & Touhami, A. E. O. (2021). Landslide susceptibility assessment using analytic hierarchy process and weight of evidence methods in parts of the Rif chain (northernmost Morocco). Arabian Journal of Geosciences, 14(14), 1346. https://doi.org/10.1007/s12517-021-07660-9
23. Fiori, E., Comellas, A., Molini, L., Rebora, N., Siccardi, F., Gochis, D. J., Tanelli, S., & Parodi, A. (2014). Analysis and hindcast simulations of an extreme rainfall event in the Mediterranean area: The Genoa 2011 case. Atmospheric Research, 138, 13–29. https://doi.org/10.1016/j.atmosres.2013.10.007
24. Funk, C., Peterson, P., Landsfeld, M., Pedreros, D., Verdin, J., Shukla, S., Husak, G., Rowland, J., Harrison, L., Hoell, A., & Michaelsen, J. (2015). The climate hazards infrared precipitation with stations—A new environmental record for monitoring extremes. Scientific Data, 2(1), 150066. https://doi.org/10.1038/sdata.2015.66
25. Gariano, S. L., & Guzzetti, F. (2016). Landslides in a changing climate. Earth-Science Reviews, 162, 227–252. https://doi.org/10.1016/j.earscirev.2016.08.011
26. Habumugisha, J. M., Chen, N., Rahman, M., Islam, M. M., Ahmad, H., Elbeltagi, A., Sharma, G., Liza, S. N., & Dewan, A. (2022). Landslide Susceptibility Mapping with Deep Learning Algorithms. Sustainability, 14(3), Article 3. https://doi.org/10.3390/su14031734
27. Hamdouni, I. E., Brahim, L. A., Mahsani, A. E., & Abdelouafi, A. (2022). The Prevention of Landslides Using the Analytic Hierarchy Process (AHP) in a Geographic Information System (GIS) Environment in the Province of Larache, Morocco. Geomatics and Environmental Engineering, 16(2), Article 2. https://doi.org/10.7494/geom.2022.16.2.77
28. Hong, H. (2023). Assessing landslide susceptibility based on hybrid Best-first decision tree with ensemble learning model. Ecological Indicators, 147, 109968. https://doi.org/10.1016/j.ecolind.2023.109968
29. Huang, F., Chen, J., Du, Z., Yao, C., Huang, J., Jiang, Q., Chang, Z., & Li, S. (2020). Landslide Susceptibility Prediction Considering Regional Soil Erosion Based on Machine-Learning Models. ISPRS International Journal of Geo-Information, 9(6), Article 6. https://doi.org/10.3390/ijgi9060377
30. Jemmah, A. I., & Brahim, L. A. (2018). Mass movement susceptibility mapping—A comparison of logistic regression and Weight of evidence methods in Taounate-Ain Aicha region (Central Rif, Morocco). MATEC Web of Conferences, 149, 02094. https://doi.org/10.1051/matecconf/201814902094
31. Jiang, Z., Chen, Y., Yang, T.-Y., Ji, W., Dong, Z.

(Sasha), & Ji, R. (2023). Leveraging Machine Learning and Simulation to Advance Disaster Preparedness Assessments through FEMA National Household Survey Data. Sustainability, 15(10), Article 10. https://doi.org/10.3390/su15108035

32. Kadavi, P. R., Lee, C.-W., & Lee, S. (2018). Application of Ensemble-Based Machine Learning Models to Landslide Susceptibility Mapping. Remote Sensing, 10(8), Article 8. https://doi.org/10.3390/rs10081252
33. Kalantar, B., Al-Najjar, H. A. H., Pradhan, B., Saeidi, V., Halin, A. A., Ueda, N., & Naghibi, S. A. (2019). Optimized Conditioning Factors Using Machine Learning Techniques for Groundwater Potential Mapping. Water, 11(9), Article 9. https://doi.org/10.3390/w11091909
34. Karmouda, N., Kacimi, I., ElKharrim, M., Brirhet, H., & Hamidi, M. (2022). Geo-statistical and hydrological assessment of three satellite precipitation products over Ouergha basin (Northern Morocco). Arabian Journal of Geosciences, 15(3), 235. https://doi.org/10.1007/s12517-021-09124-6
35. Li, G., West, A. J., Densmore, A. L., Hammond, D. E., Jin, Z., Zhang, F., Wang, J., & Hilton, R. G. (2016). Connectivity of earthquake-triggered landslides with the fluvial network: Implications for landslide sediment transport after the 2008 Wenchuan earthquake. Journal of Geophysical Research: Earth Surface, 121(4), 703–724. https://doi.org/10.1002/2015JF003718
36. Lombardo, L., Bachofer, F., Cama, M., Märker, M., & Rotigliano, E. (2016). Exploiting Maximum Entropy method and ASTER data for assessing debris flow and debris slide susceptibility for the Giampilieri catchment (north-eastern Sicily, Italy). Earth Surface Processes and Landforms, 41(12), 1776–1789. https://doi.org/10.1002/esp.3998
37. Mathbout, S., Lopez-Bustins, J. A., Royé, D., Martin-Vide, J., & Benhamrouche, A. (2020). Spatiotemporal variability of daily precipitation concentration and its relationship to teleconnection patterns over the Mediterranean during 1975–2015. International Journal of Climatology, 40(3), 1435–1455. https://doi.org/10.1002/joc.6278
38. Meena, S. R., Puliero, S., Bhuyan, K., Floris, M., & Catani, F. (2022). Assessing the importance of conditioning factor selection in landslide susceptibility for the province of Belluno (region of Veneto, northeastern Italy). Natural Hazards and Earth System Sciences, 22(4), 1395–1417. https://doi.org/10.5194/nhess-22-1395-2022
39. Merghadi, A., Yunus, A. P., Dou, J., Whiteley, J., ThaiPham, B., Bui, D. T., Avtar, R., & Abderrahmane, B. (2020). Machine learning methods for landslide susceptibility studies: A comparative overview of algorithm performance. Earth-Science Reviews, 207, 103225. https://doi.org/10.1016/j.earscirev.2020.103225
40. Michard, A., Mokhtari, A., Chalouan, A., Saddiqi, O., Rossi, P., & Rjimati, E.-C. (2014). New ophiolite slivers in the External Rif belt, and tentative restoration of a dual Tethyan suture in the western Maghrebides. Bulletin de La Société Géologique de France, 185(5), 313–328. https://doi.org/10.2113/gssgfbull.185.5.313
41. Naceur, H. A., Abdo, H. G., Igmoullan, B., Namous, M., Almohamad, H., Al Dughairi, A. A., & Al-Mutiry, M. (2022). Performance assessment of the landslide susceptibility modelling using the support vector machine, radial basis function network, and weight of evidence models in the N'fis river basin, Morocco. Geoscience Letters, 9(1), 39. https://doi.org/10.1186/s40562-022-00249-4
42. Nolasco-Javier, D., Kumar, L., & Tengonciang, A. M. P. (2015). Rapid appraisal of rainfall threshold and selected landslides in Baguio, Philippines. Natural Hazards, 78(3), 1587–1607. https://doi.org/10.1007/s11069-015-1790-y
43. Ozer, B. C., Mutlu, B., Nefeslioglu, H. A., Sezer, E. A., Rouai, M., Dekayir, A., & Gokceoglu, C. (2020). On the use of hierarchical fuzzy inference systems (HFIS) in expert-based landslide susceptibility mapping: The central part of the Rif Mountains (Morocco). Bulletin of Engineering Geology and the Environment, 79(1), 551–568. https://doi.org/10.1007/s10064-019-01548-5
44. Pal, K., & Patel, Biraj. V. (2020). Data Classification with k-fold Cross Validation and Holdout Accuracy Estimation Methods with 5 Different Machine Learning Techniques. 2020 Fourth International Conference on Computing Methodologies and Communication (ICCMC), 83–87. https://doi.org/10.1109/ICCMC48092.2020.ICCMC-00016
45. Pham, B. T., Pradhan, B., Tien Bui, D., Prakash, I., & Dholakia, M. B. (2016). A comparative study of different machine learning methods for landslide susceptibility assessment: A case study of Uttarakhand area (India). Environmental Modelling & Software, 84, 240–250. https://doi.org/10.1016/j.envsoft.2016.07.005
46. Pham, B. T., Vu, V. D., Costache, R., Phong, T. V., Ngo, T. Q., Tran, T.-H., Nguyen, H. D., Amiri, M., Tan, M. T., Trinh, P. T., Le, H. V., & Prakash, I. (2022). Landslide susceptibility mapping using state-of-the-art machine learning ensembles. Geocarto International, 37(18), 5175–5200. https://doi.org/10.1080/10106049.2021.1914746
47. Poggi, V., Garcia-Peláez, J., Styron, R., Pagani, M., & Gee, R. (2020). A probabilistic seismic hazard model for North Africa. Bulletin of Earthquake Engineering, 18(7), 2917–2951. https://doi.org/10.1007/s10518-020-00820-4

48. Poujol, A., Ritz, J.-F., Tahayt, A., Vernant, P., Condomines, M., Blard, P.-H., Billant, J., Vacher, L., Tibari, B., Hni, L., & Idrissi, A. K. (2014). Active tectonics of the Northern Rif (Morocco) from geomorphic and geochronological data. Journal of Geodynamics, 77, 70–88. https://doi.org/10.1016/j.jog.2014.01.004
49. Pourghasemi, H. R., Sadhasivam, N., Amiri, M., Eskandari, S., & Santosh, M. (2021). Landslide susceptibility assessment and mapping using state-of-the art machine learning techniques. Natural Hazards, 108(1), 1291–1316. https://doi.org/10.1007/s11069-021-04732-7
50. Prakash, B. T. P. and I. (2018). Machine Learning Methods of Kernel Logistic Regression and Classification and Regression Trees for Landslide Susceptibility Assessment at Part of Himalayan Area, India. Indian Journal of Science and Technology, 11(12), 1–10. https://doi.org/10.17485/ijst/2018/v11i12/99745
51. Prasad, A. S., & Francescutti, L. H. (2017). Natural Disasters. In S. R. Quah (Ed.), International Encyclopedia of Public Health (Second Edition) (pp. 215–222). Academic Press. https://doi.org/10.1016/B978-0-12-803678-5.00519-1
52. Qu, Y., Quan, P., Lei, M., & Shi, Y. (2019). Review of bankruptcy prediction using machine learning and deep learning techniques. Procedia Computer Science, 162, 895–899. https://doi.org/10.1016/j.procs.2019.12.065
53. Rabby, Y. W., & Li, Y. (2020). Landslide Susceptibility Mapping Using Integrated Methods: A Case Study in the Chittagong Hilly Areas, Bangladesh. Geosciences, 10(12), Article 12. https://doi.org/10.3390/geosciences10120483
54. Rahmati, O., Falah, F., Naghibi, S. A., Biggs, T., Soltani, M., Deo, R. C., Cerdà, A., Mohammadi, F., & Tien Bui, D. (2019). Land subsidence modelling using tree-based machine learning algorithms. Science of The Total Environment, 672, 239–252. https://doi.org/10.1016/j.scitotenv.2019.03.496
55. Rajaneesh, A., Vishnu, C. L., Oommen, T., Rajesh, V. J., & Sajinkumar, K. S. (2022). Machine learning as a tool to classify extra-terrestrial landslides: A dossier from Valles Marineris, Mars. Icarus, 376, 114886. https://doi.org/10.1016/j.icarus.2022.114886
56. Ramos-Bernal, R. N., Vázquez-Jiménez, R., Tizapa, S. S., Matus, R. A., Ramos-Bernal, R. N., Vázquez-Jiménez, R., Tizapa, S. S., & Matus, R. A. (2019). Characterization of Susceptible Landslide Zones by an Accumulated Index. In Landslides—Investigation and Monitoring. IntechOpen. https://doi.org/10.5772/intechopen.89828
57. Reichenbach, P., Rossi, M., Malamud, B. D., Mihir, M., & Guzzetti, F. (2018). A review of statistically-based landslide susceptibility models. Earth-Science Reviews, 180, 60–91. https://doi.org/10.1016/j.earscirev.2018.03.001
58. Roback, K., Clark, M. K., West, A. J., Zekkos, D., Li, G., Gallen, S. F., Chamlagain, D., & Godt, J. W. (2018). The size, distribution, and mobility of landslides caused by the 2015 Mw7.8 Gorkha earthquake, Nepal. Geomorphology, 301, 121–138. https://doi.org/10.1016/j.geomorph.2017.01.030
59. Roccati, A., Faccini, F., Luino, F., Ciampalini, A., & Turconi, L. (2019). Heavy Rainfall Triggering Shallow Landslides: A Susceptibility Assessment by a GIS-Approach in a Ligurian Apennine Catchment (Italy). Water, 11(3), Article 3. https://doi.org/10.3390/w11030605
60. Sadiki, M., Manaouch, M., Aghad, M., Batchi, M., & Karkouri, J. A. (2023). Identifying Landslides Prone-Areas Using GIS-based Fuzzy Analytical Hierarchy Process Model in Ziz Upper Watershed (Morocco). Ecological Engineering & Environmental Technology, 24(1), 67–83. https://doi.org/10.12912/27197050/154916
61. Saha, S., Roy, J., Pradhan, B., & Hembram, T. K. (2021). Hybrid ensemble machine learning approaches for landslide susceptibility mapping using different sampling ratios at East Sikkim Himalayan, India. Advances in Space Research, 68(7), 2819–2840. https://doi.org/10.1016/j.asr.2021.05.018
62. Salhi, A., Martin-Vide, J., Benhamrouche, A., Benabdelouahab, S., Himi, M., Benabdelouahab, T., & Casas Ponsati, A. (2019). Rainfall distribution and trends of the daily precipitation concentration index in northern Morocco: A need for an adaptive environmental policy. SN Applied Sciences, 1(3), 277. https://doi.org/10.1007/s42452-019-0290-1
63. Stoffel, M., Tiranti, D., & Huggel, C. (2014). Climate change impacts on mass movements—Case studies from the European Alps. Science of The Total Environment, 493, 1255–1266. https://doi.org/10.1016/j.scitotenv.2014.02.102
64. Tang, R.-X., Kulatilake, P. H. S. W., Yan, E.-C., & Cai, J.-S. (2020). Evaluating landslide susceptibility based on cluster analysis, probabilistic methods, and artificial neural networks. Bulletin of Engineering Geology and the Environment, 79(5), 2235–2254. https://doi.org/10.1007/s10064-019-01684-y
65. Tavakkoli Piralilou, S., Shahabi, H., Jarihani, B., Ghorbanzadeh, O., Blaschke, T., Gholamnia, K., Meena, S. R., & Aryal, J. (2019). Landslide Detection Using Multi-Scale Image Segmentation and Different Machine Learning Models in the Higher Himalayas. Remote Sensing, 11(21), Article 21. https://doi.org/10.3390/rs11212575
66. Tramblay, Y., & Somot, S. (2018). Future evolution of extreme precipitation in the Mediterranean. Climatic Change, 151(2), 289–302. https://doi.org/10.1007/s10584-018-2300-5
67. Tsunetaka, H. (2021). Comparison of the return period for landslide-triggering rainfall events in Japan

based on standardization of the rainfall period. Earth Surface Processes and Landforms, 46(14), 2984–2998. https://doi.org/10.1002/esp.5228

68. Vakhshoori, V., & Zare, M. (2016). Landslide susceptibility mapping by comparing weight of evidence, fuzzy logic, and frequency ratio methods. Geomatics, Natural Hazards and Risk, 7(5), 1731–1752. https://doi.org/10.1080/19475705.2016.1144655
69. Xie, W., Li, X., Jian, W., Yang, Y., Liu, H., Robledo, L. F., & Nie, W. (2021). A Novel Hybrid Method for Landslide Susceptibility Mapping-Based GeoDetector and Machine Learning Cluster: A Case of Xiaojin County, China. ISPRS International Journal of Geo-Information, 10(2), Article 2. https://doi.org/10.3390/ijgi10020093
70. Xing, Y., Yue, J., Guo, Z., Chen, Y., Hu, J., & Travé, A. (2021). Large-Scale Landslide Susceptibility Mapping Using an Integrated Machine Learning Model: A Case Study in the Lvliang Mountains of China. Frontiers in Earth Science, 9, 722491. https://doi.org/10.3389/feart.2021.722491
71. Yousefi, S., Pourghasemi, H. R., Emami, S. N., Pouyan, S., Eskandari, S., & Tiefenbacher, J. P. (2020). A machine learning framework for multi-hazards modeling and mapping in a mountainous area. Scientific Reports, 10(1), Article 1. https://doi.org/10.1038/s41598-020-69233-2
72. Youssef, A. M., & Pourghasemi, H. R. (2021). Landslide susceptibility mapping using machine learning algorithms and comparison of their performance at Abha Basin, Asir Region, Saudi Arabia. Geoscience Frontiers, 12(2), 639–655. https://doi.org/10.1016/j.gsf.2020.05.010
73. Zhao, B., Zhu, J., Hu, Y., Liu, Q., & Liu, Y. (2022). Mapping landslide sensitivity based on machine learning: A case study in Ankang City, Shaanxi Province, China. Geofluids, 2022, e2058442. https://doi.org/10.1155/2022/2058442
74. Zhao, P., Masoumi, Z., Kalantari, M., Aflaki, M., & Mansourian, A. (2022). A GIS-Based Landslide Susceptibility Mapping and Variable Importance Analysis Using Artificial Intelligent Training-Based Methods. Remote Sensing, 14(1), Article 1. https://doi.org/10.3390/rs14010211
75. Zhou, C., Yin, K., Cao, Y., Ahmed, B., Li, Y., Catani, F., & Pourghasemi, H.R. (2018). Landslide susceptibility modeling applying machine learning methods: A case study from Longju in the Three Gorges Reservoir area, China. Computers & Geosciences, 112, 23–37. https://doi.org/10.1016/j.cageo.2017.11.019
76. Zhou, X., Wu, W., Qin, Y., & Fu, X. (2021). Geoinformation-based landslide susceptibility mapping in subtropical area. Scientific Reports, 11(1), Article 1. https://doi.org/10.1038/s41598-021-03743-5